© 2019. This manuscript version is made available under the CC-BY-NC-ND 4.0 license http://creativecommons.org/licenses/by-nc-nd/4.0/
The published version is available via https://doi.org/10.1016/j.jcrysgro.2019.02.010.

Sublattice Reversal in GaAs/Ge/GaAs and AlAs/Ge/AlAs Heterostructures Grown on (113)A and (113)B GaAs Substrates

Xiangmeng Lu*, Yasuo Minami, Takahiro Kitada
Graduate School of Technology, Industrial and Social Sciences, Tokushima University, Tokushima 770-8506, Japan
*Corresponding author: xm-lu@tokushima-u.ac.jp

Abstract

GaAs/Ge/GaAs and AlAs/Ge/AlAs heterostructures were grown both on (113)B and (113)A GaAs substrates by molecular beam epitaxy. Sublattice reversal in these heterostructures were identified by comparing the anisotropic etching profile of the epitaxy sample with that for reference (113)B and (113)A GaAs substrates. Sublattice reversal in GaAs/Ge/GaAs heterostructures was achieved on (113)B GaAs substrate. On the other hand, sublattice reversal on (113)A GaAs substrate was obtained by using AlAs/Ge/AlAs heterostructures.

Keywords
A3. Molecular beam epitaxy; A1. Sublattice reversal; B2. GaAs/Ge/GaAs; B2. AlAs/Ge/AlAs; A1. Heterostructures; B2. (113)A and (113)B GaAs

1. Introduction

Sublattice reversal (SR) is a phenomenon that the sublattice occupation in the overgrown GaAs epitaxial layer can be changed to an opposite arrangement by inserting a thin intermediate epitaxial layer of Ge or Si in GaAs. The lattice of GaAs (0.5653 nm) and Ge (0.5658 nm) are nearly perfect matched thus GaAs/Ge/GaAs heterostructures are ideal systems for the study of SR. This growth technique has been applied to several nonlinear optical devices grown on low-index (001) or (111) GaAs substrates because SR results in sign reversal of the nonlinear optical susceptibility [1–4].

The SR in GaAs/Ge/GaAs heterostructures grown on high-index (113)B GaAs has promising application in a room-temperature terahertz (THz) device which was proposed by our group [5–7]. THz signal results from difference-frequency generation using two-color vertical-cavity surface-emitting laser around 920 nm in this device. The enhanced signal of THz was demonstrated due to the $\chi^{(2)}$ (second-order nonlinear susceptibility) inversion structure which was fabricated by face-to-face bonding of two epitaxial (113)B wafers[8]. However, it was very difficult to ensure the equivalence of optical thickness between two cavity layers because they were grown on two GaAs substrates separately. In addition, one of the substrates has to be completely removed by mechanically polishing and selective wet etching for device fabrication. This process takes a lot of time and effort. Therefore, a monolithic epitaxial technique is highly desired to achieve equivalent optical thickness of two cavity layers and avoid polishing and etching processes. SR, which results in $\chi^{(2)}$ inversion, is expected to be an alternative to wafer bonding.

We have demonstrated SR in GaAs/Ge/GaAs heterostructures on high-index (113)B GaAs substrates grown by molecular beam epitaxy (MBE) [9]. SR was further applied to a coupled multilayer cavity for THz emitter [10]. Two cavity modes with a frequency difference of 2.9 THz were clearly observed in reflection spectra. From the viewpoint of practical device applications, where THz signal results from difference-frequency generation using two-color lasers around 920 nm [11–14], AlAs/Ge/AlAs heterostructures with a higher barrier layer are required to avoid the absorption of lasers. Noted that in our previous research, SR was not achieved in GaAs/Ge/GaAs heterostructures grown on the (113)A GaAs substrate. If SR can be achieved on (113)A GaAs substrates, it means we can epitaxially grow periodically inverted $\chi^{(2)}$ structures, which are promising for quasi phase matching structures.

In this research, we comparatively investigated GaAs/Ge/GaAs and AlAs/Ge/AlAs heterostructures grown on (113)A and (113)B GaAs substrates by MBE. SR was identified by comparing the anisotropic etching profile of an epitaxial sample with those of reference (113)A and (113)B GaAs substrates. SR in GaAs/Ge/GaAs heterostructures was achieved on (113)B GaAs substrate. On the other hand, SR in AlAs/Ge/AlAs heterostructures was obtained on (113)A GaAs substrate. The mechanism of SR in GaAs/Ge/GaAs and AlAs/Ge/AlAs systems were explained by antiphase domains (APDs) self-annihilation model.

2. Experiments

Figure 1(a) illustrates the basic schematic of the SR in GaAs/Ge/GaAs grown on (113)B GaAs substrate in the ideal case. By inserting a thin intermediate layer of group-IV Ge, the sublattice occupation reversed from sublattice 1 to sublatice 2. The epitaxial structure of the GaAs/Ge/GaAs and AlAs/Ge/AlAs are shown as Figs. 1(b) and 1(c), respectively. The details of growth sequence of GaAs/Ge/GaAs were reported elsewhere [9]. The growth sequence of AlAs/Ge/AlAs was similar to that of GaAs/Ge/GaAs. A 5-nm-thick AlAs layer was grown at 600°C after growth of 500-nm-thick GaAs layer. Then, the As shouter was closed and the substrate temperature was decreased to 450°C. A 3-nm-thick Ge layer was grown at 450°C with the As source shutter closed. After the Ge growth, the As shutter was opened to establish an As prelayer. Finally, the substrate temperature was increased to 600°C for the growth of 5-nm-thick AlAs and 800-nm-thick GaAs layers.

Orientation-dependent anisotropic etching was carried out to confirm the SR. For the GaAs/Ge/GaAs as shown in the right side of Fig. 1(b), the epitaxial sample was patterned with stripes photoresist along [33-2] directions. The upper 800 nm thick GaAs layer and

the 3 nm Ge layer were etched sequentially using H_2SO_4:H_2O_2=1:10 etchant at about 3 °C and NH_4OH:H_2O_2:H_2O=2:1:100 etchant at room temperature, respectively. The lower GaAs layer was then etched under the same conditions used for the upper GaAs layer. For the AlAs/Ge/AlAs as shown in the right side of Fig. 1(c), same etchants were employed to etch GaAs and Ge layers as that of GaAs/Ge/GaAs. The etching rate of AlAs is much faster than that of GaAs in H_2SO_4:H_2O_2=1:10 etchant. Therefore, AlAs layers were etched using H_3PO_4:H_2O_2:H_2O=3:1:50 etchant at room temperature. Then the etched sample was patterned again with photoresist and the AlAs layers in the etched mesa were covered by photoresist to avoid the lateral etching along AlAs layers.

3. Results and discussion

SR was confirmed by comparing the anisotropic etching profile of an epitaxial sample with those of reference (113)A and (113)B GaAs substrates [9], which has inverse and forward mesa shapes, respectively. Cross-sectional SEM images of the anisotropic etching profiles of GaAs/Ge/GaAs grown on (113)B and (113)A GaAs substrates are shown in Figs. 2(a) and (b), respectively. The mesa shape of GaAs grown below the Ge layer (lower GaAs) was forward mesa shape, but that of GaAs grown above Ge layer (upper GaAs) was inverse mesa shape in Fig. 2(a). This result indicated that SR was achieved for the GaAs/Ge/GaAs heterostructures grown on (113)B GaAs. In contrast, SR was not achieved for the GaAs/Ge/GaAs heterostructures grown on the (113)A GaAs substrate, as shown in Fig. 2(b), where the mesas of lower and upper GaAs both have inverse mesa shapes.

Cross-sectional SEM images of the anisotropic etching profiles of AlAs/Ge/AlAs grown on (113)B and (113)A GaAs substrates are shown in Figs. 2(c) and (d), respectively.

Figs. 2(e) and 2(f) are the enlarged views of (c') in Figs. 2(c) and (d') in Figs. 2(d). SR was not achieved for the heterostructures grown on the (113)B GaAs substrate, as shown in Fig. 2(c), where the mesas of lower and upper GaAs both have forward mesa shapes. On the other hand, the SR was observed for the heterostructures grown on the (113)A GaAs substrate as shown in Fig. 2(d). The mesa shape for the lower GaAs layer is inverse mesa shape, whereas that for the upper GaAs layer is forward mesa shape.

We have demonstrated that there is no defect in the overgrown GaAs layer and directly observed the SR through the atomic arrangements by scanning transmission electron microscopy and energy-dispersive X-ray spectroscopy, respectively [10]. However, it is difficult to see the first few atomic layers from the GaAs/Ge interface, which plays a crucial role in determining whether SR occurs or not. Here, the mechanism of SR in the GaAs/Ge/GaAs system may be hypothetically explained by antiphase domains (APDs) self-annihilation model. Figure 3(a) shows a schematic illustration of the self-annihilation of APDs in GaAs grown on the Ge/GaAs layer formed on both (113)A and (113)B GaAs substrates. Antiphase boundaries (APBs) composed of (111)B As-As bond planes are generated on a Ge layer grown either on a (113)A or (113)B GaAs substrate. These APBs propagate on inclined (111) planes and encounter each other, resulting in their self-annihilation. APD associated with As-As bond planes are responsible for the observed SR in the GaAs/Ge/GaAs system on the (113)B GaAs substrate. For the case of AlAs/Ge/AlAs, the model of self-annihilation of APDs was shown in Fig. 3(b). In addition to the As-As bond planes, APBs composed of (111)A Al-Al bond planes are generated on a Ge layer grown either on both (113)A and (113)B GaAs substrates. These APBs propagate on inclined (111) planes and encounter each other, resulting in their self-annihilation. APD associated with Al-Al bond planes are responsible for the observed SR in the

AlAs/Ge/AlAs system on the (113)A GaAs substrate. These results indicated that SR was achieved both on (113)B and (113)A GaAs substrates, that is, periodically inverted $\chi^{(2)}$ structures can be epitaxially grown using GaAs/Ge/GaAs and AlAs/Ge/AlAs heterostructures.

J. Tersoff et al. have proposed a potential function which describes the motion of the IV elements with the diamond crystal structure such as germanium or silicon [15]. This potential function was further developed for a simulation of the MBE epitaxial growth for the III-V compound semiconductors [16]. The potential energy of two atoms represented by a difference between repulsive (i.e. separation) potential and attractive (i.e. bonding) potential. There is a coefficient *B* in the attractive potential term to represent the bonding strength in the simulation. For the "wrong bond" associated with APD, the *B* of Al-Al is 40.451 eV, which is smaller than that of As-As (81.32 eV), Ga-Ga (114.786 eV) and Al-Ga (69.958 eV). On the other hand, the *B* for the normal bond such as Al-As and Ga-As are 13.819 and 13.187 eV, respectively. Since the *B* for normal bonds are smaller than that of wrong bonds, it seems that the smaller the *B* is the more stable the bond is. We should be able to speculate that the Al-Al bond might more stable and favorable than Ga-Ga or As-As bonds. However, note that the numerical value of *B* was varied widely in another literature [17]. The formation of the wrong bond is a quite complex behavior which depends not only on chemical potentials but also on the charge state and interface conditions [18]. Further investigation will be required to understand the mechanism of the SR.

4. Summary

We investigated sublattice reversal in GaAs/Ge/GaAs and AlAs/Ge/AlAs heterostructures,

which were grown both on (113)B and (113)A GaAs substrates by MBE. Sublattice reversal was identified by comparing the anisotropic etching profile of the epitaxy sample with that for reference (113)A and (113)B GaAs substrates. Sublattice reversal in GaAs/Ge/GaAs heterostructures was achieved on (113)B GaAs substrate. In addition, sublattice reversal on (113)A GaAs substrate was obtained by using AlAs/Ge/AlAs heterostructures. The mechanism of SR in the GaAs/Ge/GaAs and AlAs/Ge/AlAs systems were explained by APDs self-annihilation model.

Reference

[1] S. Koh, T. Kondo, Y. Shiraki, R. Ito, GaAs/Ge/GaAs sublattice reversal epitaxy and its application to nonlinear optical devices, J. Cryst. Growth. **227–228** (2001) 183–192.

[2] S. Koh, T. Kondo, M. Ebihara, T. Ishiwada, H. Sawada, H. Ichinose, I. Shoji, R. Ito, GaAs/Ge/GaAs Sublattice Reversal Epitaxy on GaAs (100) and (111) Substrates for Nonlinear Optical Devices, Jpn. J. Appl. Phys. **38** (1999) L508–L511.

[3] A. Grisard, E. Lallier, B. Gérard, Quasi-phase-matched gallium arsenide for versatile mid-infrared frequency conversion, Opt. Mater. Express. **2** (2012) 1020–1025.

[4] T.W. Kim, K. Hanashima, T. Matsushita, T. Kondo, Antiphase structures in a periodically inverted GaAs / AlGaAs waveguide investigated by transmission electron microscopy, Jpn. J. Appl. Phys. **55** (2016) 015502.

[5] T. Kitada, F. Tanaka, T. Takahashi, K. Morita, T. Isu, GaAs/AlAs coupled multilayer cavity structures for terahertz emission devices, Appl. Phys. Lett. **95**

(2009) 111106.

[6] K. Morita, S. Katoh, T. Takimoto, F. Tanaka, Y. Nakagawa, S. Saito, T. Kitada, T. Isu, Generation of Terahertz Radiation from Two Cavity Modes of a GaAs/AlAs Coupled Multilayer Cavity, Appl. Phys. Express. **4** (2011) 102102.

[7] S. Katoh, T. Takimoto, Y. Nakagawa, K. Morita, T. Kitada, T. Isu, Terahertz Radiation from a (113)B GaAs/AlAs Coupled Multilayer Cavity Generated by Ultrashort Laser Pulse Excitation, Jpn. J. Appl. Phys. **51** (2012) 04DG05.

[8] T. Kitada, S. Katoh, T. Takimoto, Y. Nakagawa, K. Morita, T. Isu, Terahertz emission from a GaAs/AlAs coupled multilayer cavity with nonlinear optical susceptibility inversion, Appl. Phys. Lett. **102** (2013) 251118.

[9] X. M. Lu, K. Naoto, M. Yasuo, K. Takahiro, Sublattice reversal in GaAs.Ge/GaAs heterostructures grown on (113)B GaAs substrates, Appl. Phys. Express. **11** (2018) 015501.

[10] X. M. Lu, N. Kumagai, Y. Minami, T. Kitada, Sublattice reversal in GaAs/Ge/GaAs (113)B heterostructures and its application to THz emitting devices based on a coupled multilayer cavity, Jpn. J. Appl. Phys. **57** (2018) 04FH07.

[11] H. Ota, X. M. Lu, N. Kumagai, T. Kitada, T. Isu, Fabrication of two-color surface emitting device of a coupled vertical cavity structure with InAs quantum dots formed by wafer bonding, Jpn. J. Appl. Phys. **55** (2016) 04EH09.

[12] X. M. Lu, H. Ota, N. Kumagai, Y. Minami, T. Kitada, T. Isu, Two-color surface-emitting lasers by a GaAs-based coupled multilayer cavity structure for coherent terahertz light sources, J. Cryst. Growth. **477** (2017) 249–252.

[13] Y. Minami, H. Ota, X. M. Lu, N. Kumagai, T. Kitada, T. Isu, Current-injection

two-color lasing in a wafer-bonded coupled multilayer cavity with InGaAs multiple quantum wells, Jpn. J. Appl. Phys. **56** (2017) 04CH01.

[14] T. Kitada, X. M. Lu, Y. Minami, N. Kumagai, K. Morita, Room-temperature two-color lasing by current injection into a GaAs/AlGaAs coupled multilayer cavity fabricated by wafer bonding, Jpn. J. Appl. Phys. **57** (2018) 04FH03.

[15] J. Tersoff, New empirical model for the structural properties of silicon, Phys. Rev. L. **56** (1986) 632.

[16] M. Nakamura, F. Fujioka, K. Ono, M. Takeuchi, T. Mitsui, M. Oshima, Molecular dynamics simulation of III-V compound semiconductor growth with MBE, J. Cryst. Growth. **209** (2000) 232

[17] P. A. Ashu, J. H. Jefferson, A. G. Cullis, W. E. Hagston, C. R. Whitehouse, Molecular dynamics simulation of (100) InGaAs/GaAs strained-layer relaxation processes, J. Cryst. Growth. **150** (1995) 176.

[18] W. R. L. Lambercht, C. Amador, B. Segall, "Wrong" bond interactional at inversion domain boundaries in GaAs, Phys. Rev. L. **68** (1992) 1363.

Fig.1. (a) Scheme of sublattice reversal in GaAs/Ge/GaAs heterostructures. Epitaxial structure of (b) GaAs/Ge/GaAs and (c) AlAs/Ge/AlAs heterostructures.

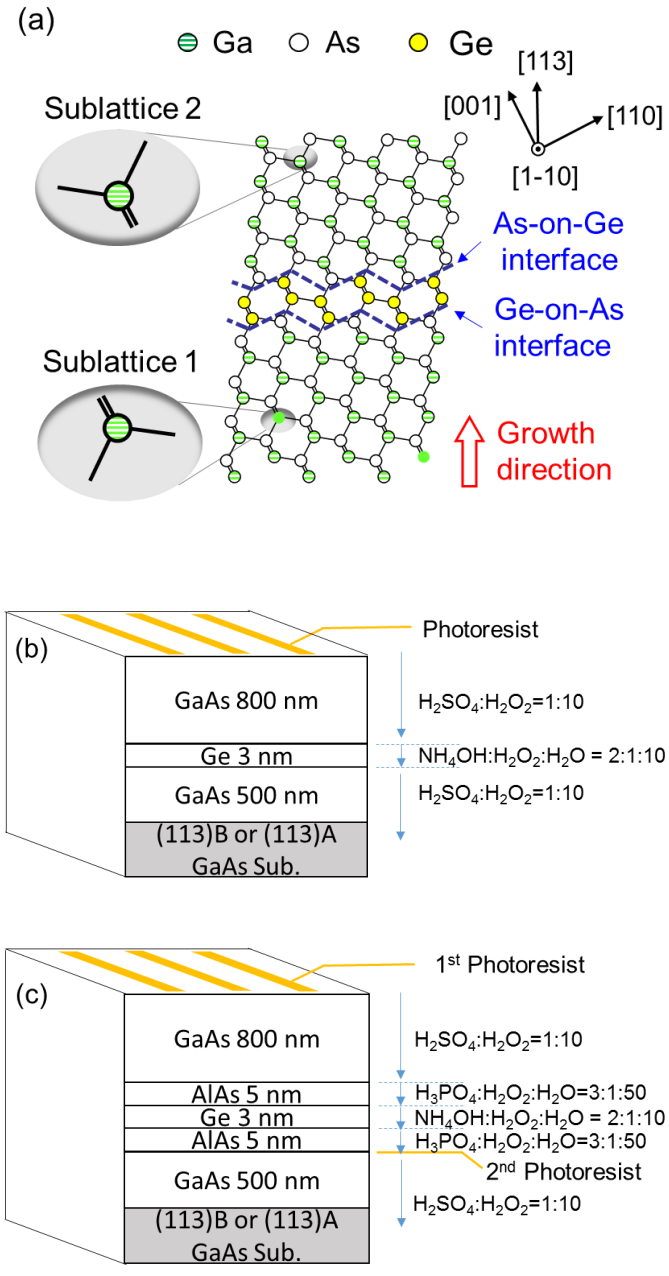

Fig.2. Cross-sectional SEM images of the anisotropic etching profiles of GaAs/Ge/GaAs grown on (a) (113)B and (b) (113)A GaAs substrates, AlAs/Ge/GaAs grown on (c) (113)B and (d) (113)A GaAs substrates. (e) and (f) are the enlarged views (c') in (c) and (d') in (d), respectively.

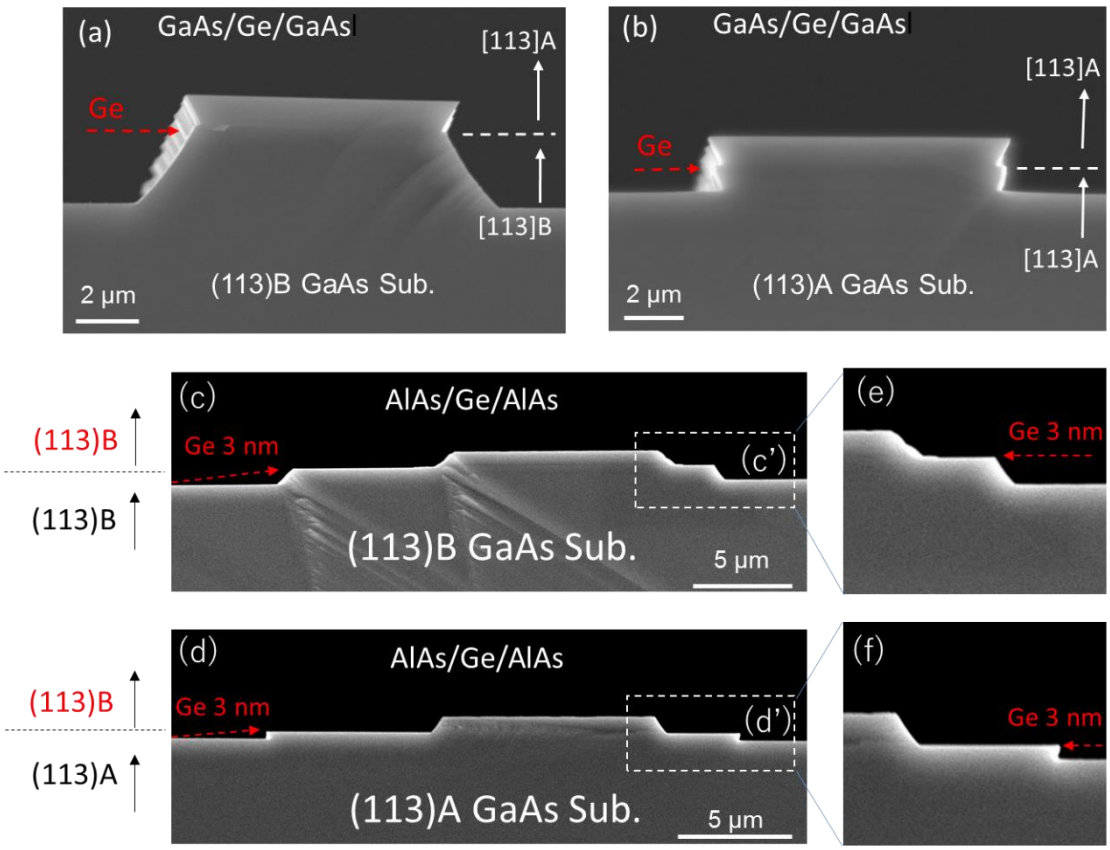

Fig. 3 Self-annihilation of APDs in (a) GaAs epilayer and (b) AlAs epilayer formed on Ge layer, which was grown on (113)A or (113)B GaAs substrates.